Available online at www.sciencedirect.com

ScienceDirect

IFAC Papers Online CONFERENCE PAPER ARCHIVE

IFAC-PapersOnLine 48-11 (2015) 097–102

Object-Oriented Modeling of a Multi-Pass Shell-and-Tube Heat Exchanger and its Application to Performance Evaluation ⋆

Javier Bonilla *,** **Margarita M. Rodríguez-García** *
Lidia Roca *,** **Loreto Valenzuela** *

* *CIEMAT-PSA, Centro de Investigaciones Energéticas, Medioambientales y Tecnológicas - Plataforma Solar de Almería, 04200, Tabernas, Almería, Spain (e-mail: javier.bonilla@psa.es, margarita.rodriguez@psa.es, lidia.roca@psa.es, loreto.valenzuela@psa.es).*
** *CIESOL, Solar Energy Research Center, Joint Institute University of Almería - CIEMAT, Almería, Spain*

Abstract: Molten salt thermal storage systems are the keystone of the dispatchability of demand in solar thermal power plants and many commercial plants use this technology. Nevertheless, there are still open questions related to long-term durability and reliability of components. During experimental campaigns in the CIEMAT-PSA molten salt testing facility, a performance detriment in a multi-pass shell-and-tube heat exchanger was noticed. For this reason and as a tool for analysis and diagnosis, an object-oriented dynamic model is being developed. This paper describes the testing facility and the thermal oil - molten salt heat exchanger particularly, the design of the Modelica model and compares simulation results against manufacturer calculations and experimental data in steady-state operation conditions and at transients in order to evaluate the heat exchanger performance.

© 2015, IFAC (International Federation of Automatic Control) Hosting by Elsevier Ltd. All rights reserved.

Keywords: object-oriented modeling, dynamic simulation, multi-pass shell-and-tube heat exchanger, thermal energy storage, molten salt, performance evaluation, Modelica.

1. INTRODUCTION

The main problem that renewable energy power plants must tackle is to provide a stable and reliable power supply. The most efficient way of storing heat through solar thermal energy, and thus dispatchability on demand, is one of the most important differences between solar thermal energy and other renewable energies (Romero-Alvarez and Zarza, 2007). This makes it appropriate for large-scale energy production while mitigating solar irradiance variability.

Nevertheless, Thermal Energy Storage (TES) systems may not be able to meet the power plant demand, specially under unfavorable meteorological conditions, due restrictions in their storage sizes because of economic reasons. Presently, this issue is overcome by hybridization with fossil fuels from which mainly emerged two technologies: integrated solar combined cycle power plants, where the solar energy contribution is relatively small (<20%) (Bohtz et al., 2013) and solar thermal power plants with auxiliary fossil fuel heaters as back-up systems, commonly dedicated to avoid the working fluid solidification but not intended to be used for electricity production (Montes et al., 2009).

Furthermore, rising cost of fossil fuels, environmental issues and concerns about sustainability are currently encouraging investment and research into multiple energy sources hybridization which may provide clean, renewable, sustainable and efficient energy. One of them is the hybridization of concentrating solar power and biomass or biogas. Biogas can be more efficiently transported through a distribution network or liquified in pressurized tanks. With this aim emerges the HYSOL project (Servert et al., 2014).

The goal of the HYSOL project is the study, design, optimization and construction of a pre-industrial demonstrator based on an innovative hybridization configuration of concentrating solar power and biogas for a 100% renewable power plant. The Manchasol parabolic-trough solar thermal power plant, owned by the HYSOL project coordinator, ACS-COBRA, is currently being adapted as a demonstrator of the HYSOL technology.

The HYSOL consortium is composed of research institutions and industrial partners. CIEMAT-PSA is the coordinator of the *dynamic modeling and advanced automatic control* work package. The dynamic model of the pre-industrial demonstrator will be used to evaluate transient responses (i.e, start-ups, shutdowns, etc.) and for the design, testing and validation of advanced control strategies. In order to calibrate and validate some dynamic models of the power plant, before its final tuning in the Manchasol plant, the CIEMAT-PSA molten salt testing facility

⋆ This research has been funded by the EU 7^{th} Framework Programme (Theme Energy 2012.2.5.2) under grant agreement 308912 - HYSOL project - Innovative Configuration of a Fully Renewable Hybrid CSP Plant and the Spanish Ministry of Economy and Competitiveness through ERDF and PLAN E funds (C.N. SolarNOVA ICT-CEPU 2009-02).

2405-8963 © 2015, IFAC (International Federation of Automatic Control) Hosting by Elsevier Ltd. All rights reserved.
Peer review under responsibility of International Federation of Automatic Control.
10.1016/j.ifacol.2015.09.166

Fig. 1. Aerial view of the molten salt testing facility (Rodríguez-García et al., 2014)

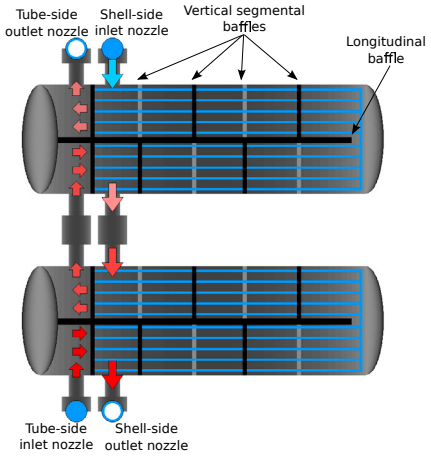

Fig. 2. Two-unit heat exchanger representation

(Rodríguez-García et al., 2014) is being used as a mock-up test bench.

This work presents the development of an object-oriented dynamic model of one of the components of the molten salt testing facility, a multi-pass shell-and-tube thermal oil - molten salt heat exchanger. During experimental campaigns, a performance detriment in this heat exchanger, with respect to design performance, was noticed. For this reason and as a tool for analysis and diagnosis, a model is being developed.

The present paper is organized as follows, section 2 describes the molten salt testing facility and the heat exchanger particularly, section 3 presents the design of the heat exchanger model, section 4 shows simulation results against manufacturer calculations at design conditions, section 5 shows performance evaluation simulations against experimental data and finally, section 6 summarizes the main conclusions and ongoing work.

2. CIEMAT-PSA MOLTEN SALT TESTING FACILITY

With the aim of studying TES systems, a multipurpose molten salt testing facility was set up at Plataforma Solar de Almería (PSA), division of CIEMAT, the public research center for Energy, Environmental and Technological Research, which is owned by the Spanish government. The main purpose of this facility is to evaluate and control the heat exchange between molten salt and different kinds of heat transfer fluids that can be used in solar thermal power plants, i.e. thermal oil and pressurized gases. For this reason the molten salt testing facility is coupled to the innovative fluids test loop facility (Rodríguez-García, 2009) by means of a CO_2 - molten salt heat exchanger. This last facility comprises two parabolic-trough collectors and allows studying pressurized gases as heat transfer fluids.

The principal components of the molten salt testing facility are listed as follows. See figure 1 to match numbers with components. For further details consult Rodríguez-García and Zarza (2011) and Rodríguez-García et al. (2014).

- *Two molten salt tanks.* Hot (1) and cold (2) molten salt tanks are in the facility in order to reproduce the sensible-heat thermal storage systems of commercial solar power plants. The cold tank is under ground level.
- *CO_2 - molten salt heat exchanger* (3). This heat exchanger can work with any other gas from the innovative fluids test loop facility.
- *Thermal oil loop.* To store and release thermal energy to/from the molten salt. The loop includes a thermal oil expansion tank, a centrifugal pump, an oil heater (8), a thermal oil - molten salt heat exchanger (5), molten salt (4) and oil (6) air coolers, an expansion tank (7) and nitrogen bottles (10) to render both fluids inert. The oil heater emulates parabolic-trough collectors by providing the same amount of heat, and also allows the plant to replicate transients such as, clouds, start-ups and shutdowns.
- *Two flanged pipe sections* (9). In these pipe sections, components can be installed and tested in the molten salt circuit under real working conditions.
- *Electrical heat-tracing system.* It was installed in order to prevent salt freezing.

There are four different operating modes in the facility. In mode 1, the molten salt TES system is charged from thermal energy coming from the innovative fluids test loop facility. Mode 2 cools down the molten salt using the air cooler system. Mode 3 charges the TES system from thermal energy coming from the thermal oil loop by means of the thermal oil - molten salt heat exchanger. Finally, mode 4 discharges the TES system by means of the same heat exchanger thus heating thermal oil.

2.1 Multi-Pass Shell-and-Tube Heat Exchanger

The thermal oil - molten salt heat exchanger is composed of two counter-flow multi-pass shell-and-tube units, see figure 2, having the molten salt in the shell side and the thermal oil in the tube side due to its high pressure.

Each unit has a TEMA-NFU (Tubular Exchanger Manufacturers Association - N-type front end stationary head, F-type shell and U-type rear end stationary head) design. The F-type shell is the most common and economical heat exchanger design used at commercial parabolic-trough solar thermal power plants (Herrmann et al., 2004). The units are tilted 2° in order to facilitate their drainage. Each one has two shell passes defined by a longitudinal

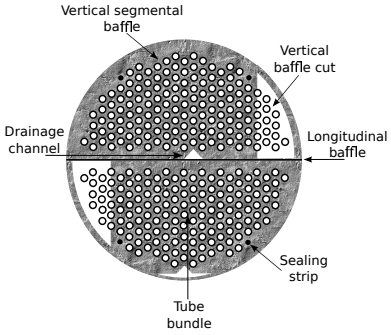

Fig. 3. Heat exchanger unit cross-sectional area

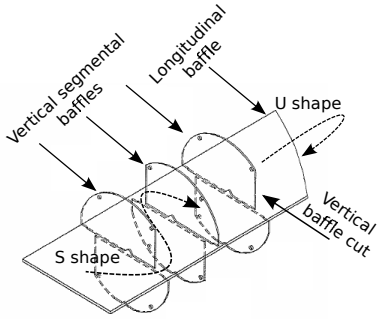

Fig. 4. S-shaped and U-shaped paths along the shell side

baffle as well as two tube passes in U shape. Some vertical segmental baffles in each shell pass, with vertical baffle cuts (see figure 3), force the shell-side fluid to follow a S-shaped path (see figure 4) in order to increase the convective heat transfer coefficient which has its highest value in cross flow. In counter flow, the tube-side fluid enters the inlet nozzle, flows along the tube bundle turning around due to the longitudinal baffle and the U-tube design, and finally leaves the heat exchanger through the outlet nozzle.

3. OBJECT-ORIENTED DYNAMIC SHELL-AND-TUBE HEAT EXCHANGER MODEL

Heat exchanger modeling has been extensively addressed in the literature because of its importance in industrial applications. Several kinds of heat exchanger models have been developed and studied targeting different aspects such as, steady-state and dynamic predictions, three-dimensional detailed and one-dimensional process models, simplified analytical models, linearized models, etc. Exhaustive reviews of heat exchangers targeting different areas are presented in Skoglund et al. (2006) and Zaversky et al. (2014). Object-oriented modeling of heat exchangers has also been studied and analyzed, Zaversky et al. (2014) provides a review addressing this topic.

The heat exchanger model presented in this work is a one-dimensional dynamic model for process simulation and control purposes. It has been developed following an object-oriented methodology based on first principles. The assumptions considered in the development of the model are summarized in the following list.

- One-dimensional dynamic model, which has been discretized in Control Volumes (CVs) by means of the Finite Volume Method (FVM) (Patankar, 1980).

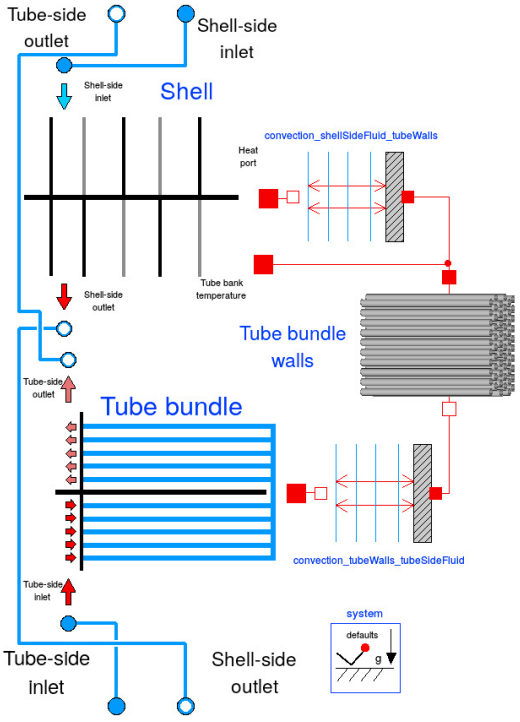

Fig. 5. Heat exchanger Modelica component diagram

- Heat conduction and radiation are negligible in the fluids. Axial heat flow in the fluids is also neglected.
- Negligible gravitational forces and differences in velocity. This leads to steady-state momentum balance formulation in both fluids where only friction forces are considered.
- Thermal conductivity in the tube walls is infinite in normal direction of flow and zero in flow direction.
- Thermal capacity of the heat exchanger shell is neglected, therefore thermal losses to the surroundings are not considered.

For the modeling of the heat exchanger, the Modelica language (Modelica Association, 2013) has been used. Modelica has been designed to model conveniently complex physical systems because the language supports the object-oriented and equation-based paradigms. The Modelica tool used for the implementation is Dymola (Dassault Systemes, 2015).

The two-unit heat exchanger Modelica icon is shown in figure 2, the number of units in series can be configured in the model. Any medium model to calculate the fluid thermodynamic properties can be used in the shell side as well as in the tube side, as long as it implements the interface of the Modelica Media library (Casella et al., 2006). Figure 5 shows the heat exchanger component diagram in Modelica.The model inputs are the inlet shell-side and tube-side temperatures and mass flow rates and, in order to close the hydraulic circuits, the outlet shell-side and tube-side pressures. The main components are described in the following sections.

3.1 Convection model

Convective heat transfer has been modeled considering the one-dimensional case of Newton's law of cooling, where the heat transfer coefficient can be dynamically calculated

from any correlation implemented in the model. In figure 5, the *convection_shellSideFluid_tubeWalls* and *convection_tubeWalls_tubeSideFluid* components model the convective heat transfer from the shell-side fluid to the tube bundle walls and from the latest to the tube-side fluid, respectively.

3.2 Shell model

This model is shown as the *shell* component in figure 5. The shell structure and dimensions have been modeled according to manufacturer data. The flow of the shell-side fluid has been modeled from the one-dimensional dynamic mass (eq. 1), dynamic energy (eq. 2) and static momentum (eq. 3) balance equations. Nomenclature is shown in table 1, the i subscript denotes the i^{th} CV. Mass and energy balance equations are discretized in CVs considering the FVM with a collocated grid (Rhie and Chow, 1983) and an upwind approach (Courant et al., 1952), whereas the static momentum balance is lumped in one equation for the whole shell and then equally distributed among the CVs. The Modelica Fluid library (Casella et al., 2006) provides base classes for the implementation of the shell model.

$$\frac{dm_i}{dt} = \dot{m}_{i,a} - \dot{m}_{i,b}, \tag{1}$$

$$\frac{dU_i}{dt} = \dot{H}_{i,a} - \dot{H}_{i,b} + \dot{Q}_i, \tag{2}$$

$$\Delta p_i = p_{i,a} - p_{i,b}. \tag{3}$$

Medium. Owing to the fact that in the Modelica Media library there are no media for molten salts, solar salt (60% $NaNO_3$ and 40% KNO_3) thermodynamic properties have been implemented. Its thermodynamic properties are available in Ferri et al. (2008) and Zavoico (2001).

Heat transfer. The heat transfer coefficient between the shell-side fluid and the outer tube bundle walls can be calculated by two correlations in the model, both for forced convection and turbulent flow. The first one is that proposed by Gaddis and Gnielinski (VDI, 2010), this correlation takes into account geometrical parameters as well as leakage and bypass correction factors. The other correlation is that proposed in Serth (2007), this one is a curve fit from data provided in Kraus et al. (2002). Better results were obtained with the second correlation and therefore this is the one currently used in the model.

Pressure drop. The pressure drop model is that proposed in Gaddis (1997) and VDI (2010) for shell-and-tube heat exchangers with segmental baffles. This model takes into account the pressure drop at cross-flow (parallel to vertical baffles) and window (across vertical baffles through baffle cuts) sections as well as at the inlet and outlet nozzles.

3.3 Tube bundle model

This model is shown as the *tube bundle* component in figure 5. The flow of the tube bundle fluid has been modeled in the same way as the shell model, i.e. considering eqs. 1, 2 and 3. Additionally, the number of parallel CVs is a parameter of the model, this allows to consider the number of tubes in the bundle.

Table 1. Nomenclature

Variable	Description		Units
c_p	Specific heat capacity		[J/(kg·K)]
$\dot{H}$	Enthalpy flow rate		[W]
m	Mass		[kg]
$\dot{m}$	Mass flow rate		[kg/s]
p	Pressure		[Pa]
$\dot{Q}$	Heat flow rate		[W]
T	Temperature		[K]
t	Time		[s]
U	Internal energy		[J]
Subscript	Description	Subscript	Description
a	Inlet	b	Outlet

Medium. Therminol VP-1 thermodynamic properties have been implemented according to Solutia (2008).

Heat transfer. Three correlations are available for internal forced convection when considering turbulent, transitional or laminar flow: Gnielinski (1976), Hausen (1943) and Sieder and Tate (1936), respectively.

Transition between coefficients has been smoothed, according to the approach presented in Richter (2008) and with the intervals described in Zaversky et al. (2013), in order to be continuous during simulation and thus avoiding numerical integration problems.

Pressure drop. A detailed model from the Modelica Fluid library, which considers all possible cases in the Moody diagram (Moody, 1944), has been used. Pressure loss at nozzles has been modeled according to VDI (2010), whereas pressure loss in the U-shaped elbows is small and therefore it has been neglected.

3.4 Tube bundle wall model

This model (the *tube bundle walls* component in figure 5) considers the energy balance equation (eq. 4). The model has been discretized in CVs in the same way as the *shell* and *tube bundle* models. The number of parallel tubes can be also configured in this model.

$$m_i c_{p,i} \frac{dT_i}{dt} = \dot{Q}_i. \tag{4}$$

Density and specific heat capacity values have been obtained from data sheets (A-106 grade B carbon steel pipe) and they can be configured as average constant values or interpolated values as a function of temperature.

4. SIMULATION AT DESIGN CONDITIONS

In order to verify the model, design performance calculations provided by the manufacturer were compared to simulation results at design conditions: inlet molten salt temperature 290 °C, mass flow rate 7472 kg/h and pressure 2 bar, and inlet thermal oil temperature 380 °C, mass flow rate 5654 kg/h and pressure 14 bar. DASSL (Petzold, 1983) has been the numerical integrator used for the simulations performed in Dymola.

Manufacturer calculations together with simulation results, considering different numbers of CVs, are shown in table 2. It can be seen that simulation results agree with the performance calculation provided by the manufacturer.

Table 2. Simulation results at design conditions

	Design	Simulation		
		25 CVs	50 CVs	75 CVs
Compilation time (s)	-	7	13	20
Simulation time (s)	-	0.36	1.16	2.39
Spatial resolution [1] (m)	-	2.02	1.01	0.67
Heat exchanged (kW)	257.5	252.27	256.08	257.36
Shell side - Molten salt				
Outlet temp. (°C)	373	371.04	372.26	372.67
Temp. difference (°C)	-	1.96	0.74	0.33
Pressure drop (bar)	0.4	0.4543	0.4537	0.4535
Tube side - Thermal oil				
Outlet temp. (°C)	313	314.56	313.53	313.19
Temp. difference (°C)	-	1.56	0.53	0.19
Pressure drop (bar)	0.03	0.0308	0.0310	0.0311

5. PERFORMANCE EVALUATION SIMULATIONS

Once the model has been verified against design data, the next step is to compare the response of the model against steady-state and transient experimental data.

A stationary experiment at design conditions in operating mode 3 (heating up molten salt) is presented in this section. Figure 6 shows experimental inlet molten salt temperature as well as experimental and simulated outlet molten salt temperatures, where mass flow rates and pressures were set close to design conditions (cf. section 4). Same information is shown in figure 7, but in this case for thermal oil. It can be seen, from both figures, that the performance of the heat exchanger is lower than the theoretical one.

Considering experimental data from several operating days and after studying and analyzing the results, they reveal that the thermal oil transfers 6.5% less thermal energy that the theoretical one on average and the molten salt receives 26% less thermal energy than that considered in the design of the heat exchanger. This performance detriment, together with experimental data, was used to adjust the model and the results are also shown in figures 6 and 7, as adjusted simulated outlet temperatures. The accuracy of the K-type class 2 thermocouples installed in the facility, which were calibrated in accordance with the International Electrotechnical Commission (IEC) 584.3 norm, is ±3 °C. In this steady-state comparison, the maximum temperature difference between experimental and adjusted simulated outlet temperatures, for both fluids, is lower than 3.5 °C, being the mean absolute deviation of 1.6 °C.

The transient response of the model is also being evaluated. Figures 8 and 9 show experimental inlet temperature as well as experimental and simulated outlet temperatures for the molten salt and thermal oil in an operating mode 3 experiment which reproduces cloud disturbances in the solar field. Clouds were replicated by reducing the inlet thermal oil temperature in the oil heater and then setting it back to its original value, as it can be seen in figure 9. The dynamic response of the model, taking into account the performance detriment previously estimated, shows a good agreement with experimental data in both, outlet thermal oil temperature as well as outlet molten salt temperature. The maximum difference between experimental and simulated outlet temperatures is lower than 5 °C for

[1] Taking into account the S-shaped and U-shaped paths

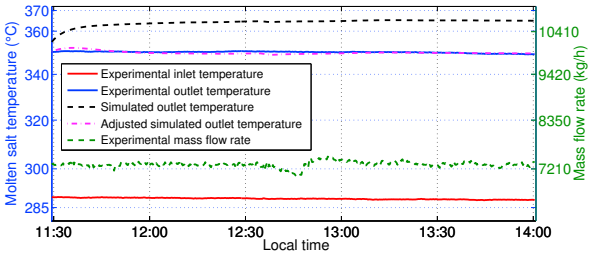

Fig. 6. Molten salt temperatures in steady state

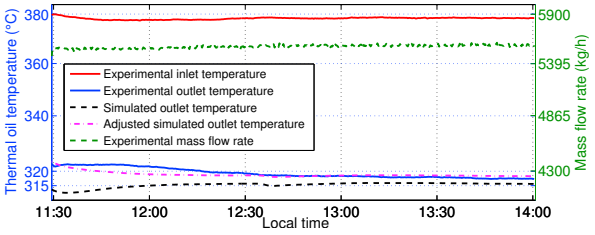

Fig. 7. Thermal oil temperatures in steady state

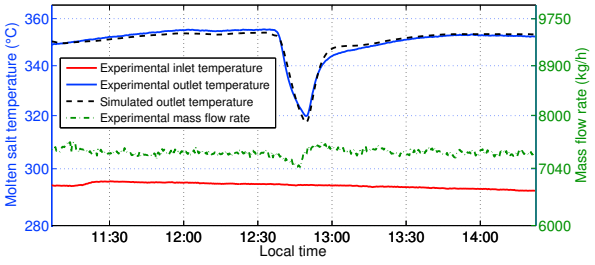

Fig. 8. Molten salt temperatures at transient

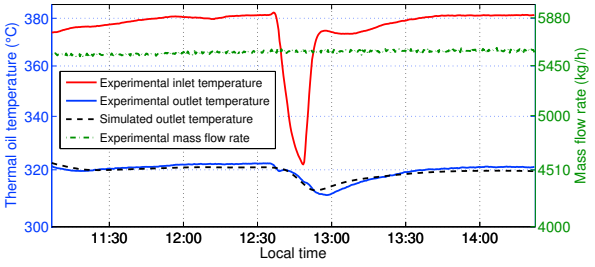

Fig. 9. Thermal oil temperatures at transient

both fluids. The mean absolute deviation is lower than 2.6 °C. The following step will be to identify the causes for the heat exchanger performance detriment. The most common causes for deterioration in performance of F-shell heat exchangers are thermal leakage or physical leakage due to the longitudinal baffle (Mukherjee, 2004) together with fouling, corrosion, design errors and fabrication issues. Additionally, two potential issues were identified with this heat exchanger, as presented in Rodríguez-García et al. (2014). One of them is the bypass of molten salt through the drainage channels (see figure 3) and the other one is the nitrogen accumulation inside the shell due to the heat exchanger tilt angle. Both might decrease the heat transfer area between the molten salt and the tube bundle. All these issues will be analyzed and implemented in the model in order to determine which of them causes the performance detriment in the real system.

6. CONCLUSIONS AND FUTURE WORK

This paper has presented a preliminary object-oriented dynamic multi-pass shell-and-tube heat exchanger model. Simulation results have been compared against experimental data from the CIEMAT-PSA molten salt testing facility in steady-state conditions and transient predictions. Finally, the performance detriment of the heat exchanger has been estimated.

Ongoing work includes a more detailed heat exchanger model considering all mentioned causes for deterioration in performance to identify them in the real system, as well as performing experimental campaigns in operating modes 3 and 4, covering the whole operating range, in order to adjust, calibrate and validate the transient response of the dynamic model.

REFERENCES

Bohtz, C., Gokarn, S., and Conte, E. (2013). Integrated Solar Combined Cycles (ISCC) to Meet Renewable Targets and Reduce CO_2 Emissions. In *PowerGen Europe*, 20. Vienna, Austria.

Casella, F., Otter, M., Proelss, K., Richter, C., and Tummescheit, H. (2006). The Modelica Fluid and Media library for modeling of incompressible and compressible thermo-fluid pipe networks. In *Proc. 5th International Modelica Conference*, 631–640. Vienna, Austria.

Courant, R., Isaacson, E., and Rees, M. (1952). On the solution of nonlinear hyperbolic differential equations by finite differences. *Communications on Pure and Applied Mathematics*, 5, 243–255. doi:10.1002/cpa.3160050303.

Dassault Systemes (2015). Dymola 2015 - Multi-Engineering Modeling and Simulation. URL `http://www.dymola.com`.

Ferri, R., Cammi, A., and Mazzei, D. (2008). Molten salt mixture properties in RELAP5 code for thermodynamic solar applications. *International Journal of Thermal Sciences*, 47(12), 1676–1687. doi: 10.1016/j.ijthermalsci.2008.01.007.

Gaddis, S. (1997). Pressure drop on the shell side of shell-and-tube heat exchangers with segmental baffles. 36, 149–159. doi:10.1016/S0255-2701(96)04194-3.

Gnielinski, V. (1976). New equations for heat and mass transfer in turbulent pipe flow and channel flow. *International Chemical Engineering*, 2(16), 359–368.

Hausen, H. (1943). Darstellung des Wärmeüberganges in Rohren durch verallgemeinerte Potenzbeziehyngen. *VDI - Verfahrenstechnik*, 4, 91–98.

Herrmann, U., Kelly, B., and Price, H. (2004). Two-tank molten salt storage for parabolic trough solar power plants. *Energy*, 29(5-6), 883–893. doi:10.1016/S0360-5442(03)00193-2.

Kraus, A.D., Aziz, A., and Welty, J. (2002). *Extended Surface Heat Transfer*. Wiley.

Modelica Association (2013). Modelica Standard Library 3.2.1. URL `http://www.modelica.org`.

Montes, M., Abánades, A., Martínez-Val, J., and Valdés, M. (2009). Solar multiple optimization for a solar-only thermal power plant, using oil as heat transfer fluid in the parabolic trough collectors. *Solar Energy*, 83(12), 2165–2176. doi:10.1016/j.solener.2009.08.010.

Moody, L. (1944). Friction factors for pipe flow. *Transactions of the ASME*, 66, 671–684.

Mukherjee, R. (2004). Does Your Application Call for an F-Shell Heat Exchanger? *CEP magazine*, (April), 40–45.

Patankar, S. (1980). *Numerical Heat Transfer and Fluid Flow*. Hemisphere, Washington D.C.

Petzold, L. (1983). A description of DASSL: a Diferential/Algebraic System Solver. *Scientific Computing*, 65–68.

Rhie, C.M. and Chow, W.L. (1983). Numerical study of the turbulent flow past an airfoil with trailing edge separation. *The American Institute of Aeronautics and Astronautics Journal*, 21, 1525–1532.

Richter, C. (2008). *Proposal of New Object-Oriented Equation-Based Model Libraries for Thermodynamic Systems*. Ph.D. thesis, Technische Universität Carolo-Wilhelmina zu Braunschweig, Germany.

Rodríguez-García, M.M. (2009). First Experimental Results of a PTC Facility Using Gas as the Heat Transfer Fluid. In *15th SolarPACES Conference*. Berlin, Germany.

Rodríguez-García, M.M., Herrador-Moreno, M., and Zarza Moya, E. (2014). Lessons learnt during the design, construction and start-up phase of a molten salt testing facility. *Applied Thermal Engineering*, 62(2), 520–528. doi:10.1016/j.applthermaleng.2013.09.040.

Rodríguez-García, M.M. and Zarza, E. (2011). Design and Construction of an Experimental Molten Salt Test Loop. In *17th SolarPACES Conference*. Granada, Spain.

Romero-Alvarez, M. and Zarza, E. (2007). Concentrating Solar Thermal Power. In *Handbook of Energy Efficiency And Renewable Energy*, chapter 21, 1–98. CRC Press.

Serth, R.W. (2007). *Process Heat Transfer: Principles and Applications*. Elsevier Science.

Servert, J., Cerrajero, E., López, D., Yagüe, S., Gutierrez, F., Lasheras, M., and San Miguel, G. (2014). Base Case Analysis of a HYSOL Power Plant. In *20th SolarPACES Conference*. Beijing, China.

Sieder, E.N. and Tate, G.E. (1936). Heat Transfer and Pressure Drop of Liquids in Tubes. *Industrial & Engineering Chemistry*, 28(12), 1429–1435. doi: 10.1021/ie50324a027.

Skoglund, T., Arzen, K., and Dejmek, P. (2006). Dynamic object-oriented heat exchanger models for simulation of fluid property transitions. *International Journal of Heat and Mass Transfer*, 49(13-14), 2291–2303. doi: 10.1016/j.ijheatmasstransfer.2005.12.005.

Solutia (2008). Therminol VP-1 heat transfer fluid - Vapour and Liquid phases. Technical bulletin 7239115C.

VDI (2010). *VDI Heat Atlas*. Springer, 2nd edition.

Zaversky, F., García-Barberena, J., Sánchez, M., and Astrain, D. (2013). Transient molten salt two-tank thermal storage modeling for CSP performance simulations. *Solar Energy*, 93, 294–311. doi: 10.1016/j.solener.2013.02.034.

Zaversky, F., Sánchez, M., and Astrain, D. (2014). Object-oriented modeling for the transient response simulation of multi-pass shell-and-tube heat exchangers as applied in active indirect thermal energy storage systems for concentrated solar power. *Energy*, 65, 647–664. doi: 10.1016/j.energy.2013.11.070.

Zavoico, A.B. (2001). Solar Power Tower - Design Basis Document. Technical Report SAND2001-2100, Sandia National Laboratories, Albuquerque, USA.